

# Theoretical investigations on the synthesis mechanism of cyanuric acid from $\text{NH}_3$ and $\text{CO}_2$

Xueli Cheng · Yanyun Zhao · Weiqun Zhu · Yongjun Liu

Received: 4 July 2013 / Accepted: 8 September 2013 / Published online: 29 September 2013  
© Springer-Verlag Berlin Heidelberg 2013

**Abstract** In the synthesis of cyanuric acid from  $\text{NH}_3$  and  $\text{CO}_2$ , urea and isocyanic acid OCNH are two pivotal intermediates. Based on density functional theory (DFT) calculations, the synthesis mechanism of cyanuric acid from  $\text{NH}_3 + \text{CO}_2$  was investigated systematically. Urea can be synthesized from  $\text{NH}_3$  and  $\text{CO}_2$ , and cyanuric acid can be obtained from urea or  $\text{NH}_3 + \text{CO}_2$ . In the stepwise mechanism of cyanuric acid from urea or  $\text{NH}_3 + \text{CO}_2$ , the energy barriers are relatively high, and the condition of high pressure and temperature does not decrease the energy barriers. Our theoretical model shows that cyanuric acid is actually acquired from OCNH via a one-step cycloaddition reaction.

**Keywords** Cyanuric acid ·  $\text{NH}_3$  and  $\text{CO}_2$  · Urea · Density functional theory · Mechanism

## Introduction

Since cyanuric acid and melamine were reported publicly to have been added illegally to dairy products and pet foods in China to increase the nitrogen content [1–5], they are almost regarded as detrimental and hazardous chemicals by the common Chinese populace. However, cyanuric acid, melamine

and their derivatives are a class of representative heterocyclic compounds with unique physical and chemical properties [6–8]. Cyanuric acid is also an important chemical material and chemical intermediate [9]. Its most important feature is that it can be synthesized from small molecules such as ammonia and carbon dioxide with or without catalysts and solvents [10–13], and the products are cyanuric acid and water. It is well known that carbon dioxide is the main greenhouse gas (GHG) and the major contributing factor to recent global warming, so this green process also plays an important role in the efficient utilization of the abundant and renewable  $\text{CO}_2$  resource in an environmentally friendly manner [14].

Urea can also be synthesized from  $\text{NH}_3$  and  $\text{CO}_2$  [11, 14–16], and then cyanuric acid synthesized from urea [3, 17]. Urea and isocyanic acid [10, 15, 18, 19] are key intermediates in the synthesis of cyanuric acid from  $\text{NH}_3$  and  $\text{CO}_2$ . It has been reported that cyanuric acid can be acquired from urea  $\text{CO}(\text{NH}_2)_2$  [20]. The Wöhler synthesis of urea from  $\text{NH}_3$  and  $\text{CO}_2$  is a chemical classic, and the pioneering work of Tsipis and Karipidis [11, 16] has reported systematical density functional theory (DFT) calculations on the formation of urea from  $\text{NH}_3$  and  $\text{CO}_2$  at B3LYP/6-31G(d,p) level. However, to the best of our knowledge, there are no experimental and theoretical mechanistic investigations on the formation of cyanuric acid from urea or  $\text{NH}_3 + \text{CO}_2$ . The synthetic mechanism of cyanuric acid from  $\text{NH}_3$  and  $\text{CO}_2$  in the absence of any catalysts or solvents needs further theoretical investigation, and the influence of high temperature and high pressure in the synthesis of cyanuric acid remain unknown. In the present work, we carried out a theoretical investigation on the gas-phase synthesis mechanisms of cyanuric acid from  $\text{NH}_3$  and  $\text{CO}_2$  free of any ligands, solvents and support effects with DFT methods, and consider the influence of temperature and pressure to confirm the reactivity of urea and isocyanic acid in this reaction system.

**Electronic supplementary material** The online version of this article (doi:10.1007/s00894-013-2003-9) contains supplementary material, which is available to authorized users.

X. Cheng · W. Zhu · Y. Liu (✉)  
School of Chemistry and Chemical Engineering,  
Shandong University, Jinan 250100, China  
e-mail: yongjunliu\_1@sdu.edu.cn

X. Cheng (✉) · Y. Zhao  
School of Chemistry and Chemical Engineering, Taishan University,  
Tai'an 271021, China  
e-mail: ching108@sohu.com

## Computational methods

The hybrid density functionals such as B3LYP are the most versatile theoretical methods, and have already been applied successfully to a variety of urea and ammonia systems [11, 16, 21–24]. The reactants, intermediates and products were fully optimized at B3LYP/6-311++G(d,p) level with the Gaussian 03 program package [25] in the present work. Frequency calculations were also performed at the same level to identify whether the stationary point is a local minimum or a transition state. Furthermore, the displacement vectors of the imaginary vibrational modes were used to identify real transition states and their connections [26]. Based on the optimized structures of intermediates or reactants, we adjusted the bond distances and bond angles to guess the initial structures of transition states, and then employed the `opt=(calcfc,ts,noeigentest)` keyword to request full optimization to transition states rather than a local minimum using the Berny algorithm and to specify that the force constants be computed at the first point [27]. The transition state structures all represent saddle points, characterized by one and only one negative eigenvalues of the Hessian matrix. Some key transition states were further checked by intrinsic reaction coordinate (IRC) calculations to confirm their connections between the corresponding intermediates [28, 29]. It is well known that cyanuric acid is synthesized from  $\text{NH}_3$  and  $\text{CO}_2$  under high pressure and temperature [11, 16]. To better simulate the reaction conditions, single-point energy (SPE) calculations with the keyword `Freq=ReadIsotopes` were carried out to recompute the thermodynamic functions at 473.15 K and 100 atm. This temperature is much higher than the critical temperatures of  $\text{NH}_3$  and  $\text{CO}_2$  (132.4 and 31.0 °C, respectively), so the classical rigid rotator model and harmonic oscillator model were employed in this work.

## Results and discussion

The lowest frequencies and their vibrational mode assignments as well as the differences of electronic and zero-point energies ( $\Delta E$ ), Gibbs free energies ( $\Delta G$ ) and thermal enthalpies ( $\Delta H$ ) at 473.15 K and 100 atm of all species involving this reaction system are listed in Table S1 of Supporting Information. High pressure and high temperature can alter the values of Gibbs free energies ( $G$ ), thermal energies ( $U$ ) and thermal enthalpies ( $H$ ), so, in the present work, we used  $\Delta G$  values to elucidate the reaction mechanisms.

To validate the reliability of the B3LYP method, the addition of  $\text{NH}_3$  and  $\text{CO}_2$  to form carbamic acid ( $\text{NH}_2\text{COOH}$ ) was also fully optimized with the second order approximation of Møller-Plesset perturbation theory (MP2) at 6-311++G(d,p) basis set level, and we found that the MP2 energies and

structural parameters are in excellent agreement with those of B3LYP. Based on the B3LYP-optimized structural parameters, for the addition of  $\text{NH}_3$  and  $\text{CO}_2$ , the SPE calculations were carried out at CCSD(T)/aug-cc-pVDZ level with frequency calculations to obtain the thermodynamic functions at 473.15 K and 100 atm. Again, the CCSD(T) free energies are comparable with the B3LYP and MP2 values, but the barrier is lower than the B3LYP or MP2 barrier because the CCSD(T) relative energy of **IM1** is relatively higher, as shown in Fig. 1. We will now discuss the stepwise mechanism with the B3LYP results.

The initial step :  $\text{NH}_3 + \text{CO}_2 \rightarrow \text{OCNH} + \text{H}_2\text{O}$

The reactions of  $\text{NH}_3 + \text{CO}_2$  leading to  $\text{OCNH} + \text{H}_2\text{O}$  are depicted in Fig. 1. Firstly,  $\text{NH}_3$  bonds to  $\text{CO}_2$  to form a weak van der Waals complex **IM1**. The interaction mode, which is similar to the bonding between methylenimine and isocyanic acid  $\text{OCNH}$  [30], was revealed by Tshipis and Karipidis [16]. The MP2 geometrical parameters of **IM1** [31] are also in excellent agreement with our results. **IM1** transforms to **IM2** via a hydrogen-shift transition state **TS1**, followed by an isomerization process and another H-shift process, ultimately leading to isocyanic acid  $\text{OCNH}$  and  $\text{H}_2\text{O}$ . These processes were investigated in the pioneering work of Tshipis and Karipidis [16], which agrees well with our calculation results. The  $\Delta H$  values show that the formation of **IM3** is slightly endothermic, but the formation of  $\text{OCNH} + \text{H}_2\text{O}$  requires a heat of  $78.6 \text{ kJ/mol}^{-1}$ , as shown in Table S1.

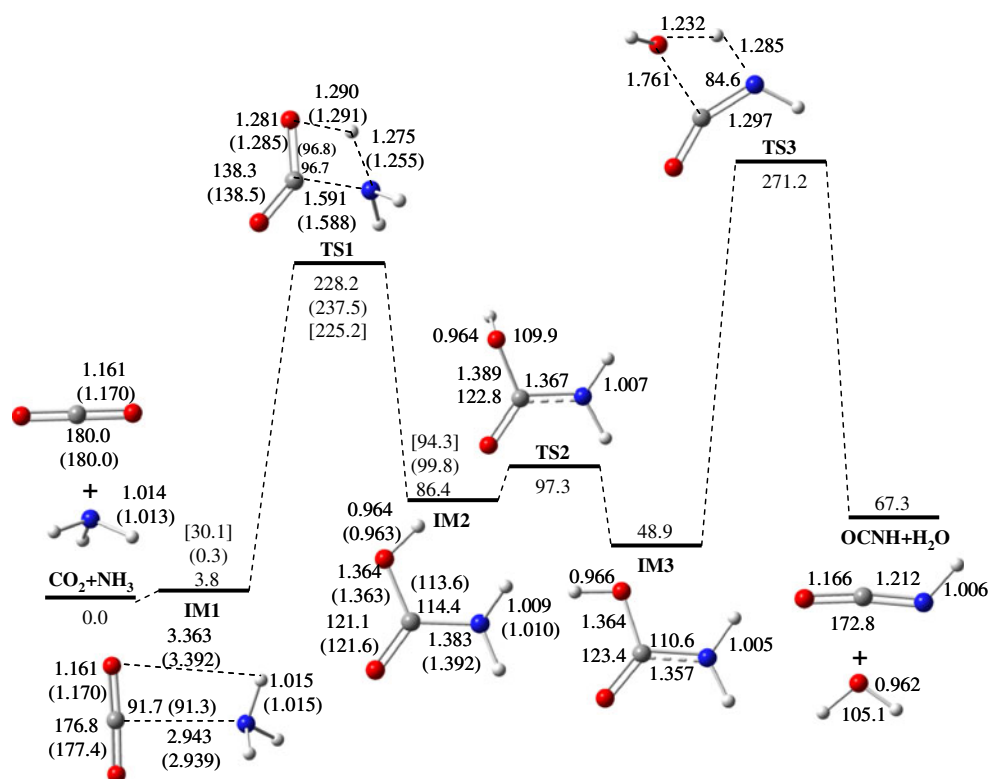
$\text{OCNH}$  is a key intermediate, and its reactions with small molecules such as  $\text{H}_2\text{O}$  [31, 32], allenes [33],  $\text{HCOOH}$  [34] and  $\text{NH}_3$  [11, 35] have been studied theoretically. Figure 1 shows that the free energy barrier of  $\text{OCNH}$  generation is as high as  $222.3 \text{ kJ/mol}^{-1}$ . Moreover, Tshipis and Karipidis [11] elucidated the reaction mechanism of  $\text{OCNH} + \text{NH}_3$  to urea with a total barrier ( $\Delta E$ ) of  $161.9 \text{ kJ/mol}^{-1}$ .

We also investigated whether an additional  $\text{NH}_3$  molecule can serve as a catalyst to decrease the free energy barrier of the addition reaction of  $\text{NH}_3$  and  $\text{CO}_2$  (Fig. 2). Two  $\text{NH}_3$  molecules links to  $\text{CO}_2$  via a six-membered ring to produce **IM1'**, and then a hydrogen atom on  $\text{NH}_3$  transfers to O via **TS1'**. Although the barrier is reduced slightly to  $195.1 \text{ kJ/mol}^{-1}$ , the relative free energy of **TS1'** ( $225.2 \text{ kJ/mol}^{-1}$ ) does not decrease apparently compared with **TS1** ( $228.2 \text{ kJ/mol}^{-1}$ ). As a result, the influence of additional  $\text{NH}_3$  molecules will not be considered further in the present work.

**IM3** +  $\text{NH}_3$  : Formation of rea and another channel producing  $\text{OCNH}$

Then, another  $\text{NH}_3$  molecule links to **IM3** and one hydrogen atom transfers from  $\text{NH}_3$  to hydroxyl oxygen via **TS4** to produce urea by dehydration (Fig. 3a). From IRC scanning we obtain a quaint intermediate **IM4** before hydrogen transfer, as

**Fig. 1** Structural parameters and potential energy surface (PES) profiles of  $\text{NH}_3 + \text{CO}_2 \rightarrow \text{OCNH} + \text{H}_2\text{O}$ . Red circles Oxygen atoms, blue circles nitrogen atoms. Relative free energies ( $\Delta G$ ) are in  $\text{kJ mol}^{-1}$ , bond lengths are in Å and bond angles in degrees. Structural parameters and relative energies in brackets ( ) are acquired from full optimization at MP2/6-311++G(d,p) level, and energies in square brackets [ ] are obtained by SPE calculations at CCSD(T)/aug-cc-pVDZ level. These units are employed uniformly in this work, and all energies are relative to the reactants ( $3\text{NH}_3 + 3\text{CO}_2$ ) in all figures



reported by Tsepis and Karipidis [16]. The frontier orbitals reveal why ammonia nitrogen attacks the imine hydrogen via hydrogen bonding rather than the carbon atom, as shown in Fig. 3b. The hydrogen atom then transfers from  $\text{NH}_3$  to the hydroxyl group via **TS4** with a barrier of  $269.5 \text{ kJ mol}^{-1}$ ,

yielding **IM5**, which will decompose into urea and  $\text{H}_2\text{O}$  via a barrierless process.

From **IM5**, there is another reaction channel generating **OCNH**, i.e., an imine hydrogen atom transfers to another imine group to form urea mediated by  $\text{H}_2\text{O}$ , as shown in Fig. 3. The free energy barrier is only  $123.0 \text{ kJ mol}^{-1}$ , much lower than that of the **IM3** dehydrating process producing **OCNH**. From Fig. 3 it can also be seen that urea can transform to **OCNH** with a relatively low barrier. Therefore, the generation of **OCNH** from urea and  $\text{H}_2\text{O}$  is energetically favorable.

#### Addition reaction of urea + $\text{CO}_2$

This addition reaction is very analogous to the reaction of  $\text{NH}_3 + \text{CO}_2$ , as shown in Fig. 4.  $\text{CO}_2$  can be added to an amido group of urea to form **IM8**, but the bond distance of the newly formed C–N (3.233 Å) in **IM7** is much longer than that in **IM1** (2.943 Å). A hydrogen atom on the amino group then shifts to the oxygen atom of  $\text{CO}_2$ , and the carbon atom of  $\text{CO}_2$  bonds simultaneously to the N atom via **TS6** to form **IM8**. The only imaginary frequency of **TS6** is assigned to the C–N–H asymmetrical stretch mode, and the bond lengths between the shifting hydrogen atom and O, N are 1.284 and 1.283 Å. The energy barrier of this addition reaction is relatively high ( $240.0 \text{ kJ mol}^{-1}$ ).

There are two reaction pathways starting from **IM8**. We can add carbon dioxide to another imine group, or add  $\text{NH}_3$  to the carboxyl group. Now we investigate the reaction mechanism of

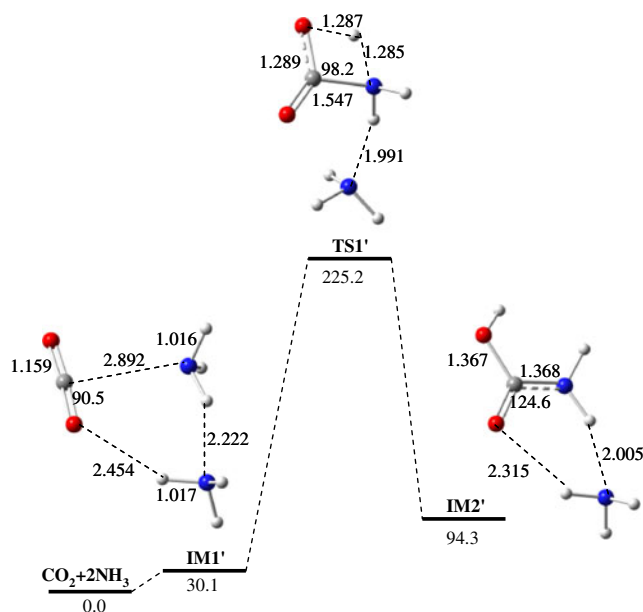


**Fig. 2** Structural parameters and PES profile of  $2\text{NH}_3 + \text{CO}_2 \rightarrow \text{OCNH-NH}_3 + \text{H}_2\text{O}$

**Fig. 3** **a** Structural parameters and PES profile of  $\text{IM3}+\text{NH}_3 \rightarrow \text{OCNH} + \text{H}_2\text{O} + \text{NH}_3$ . **b** HOMO–LUMO interaction during the formation of complex  $\text{IM3} \dots \text{NH}_3$  ( $\text{IM4}$ )

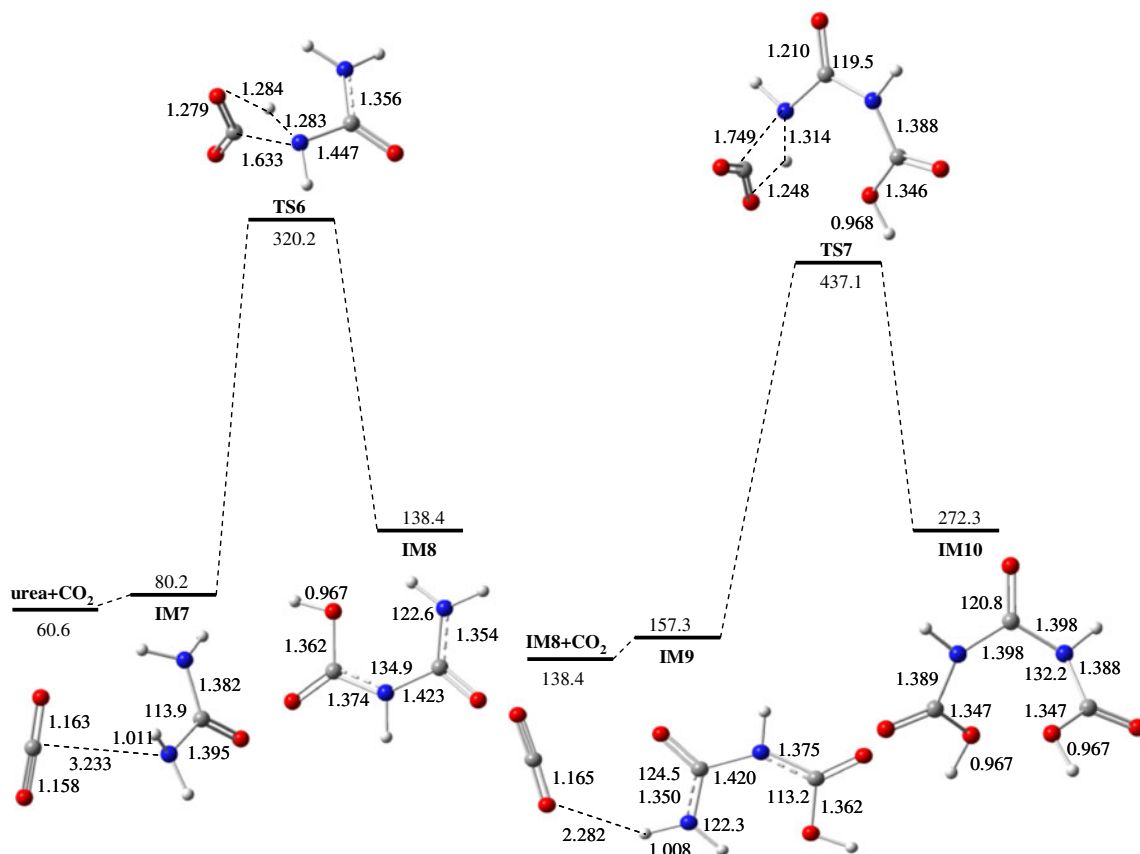
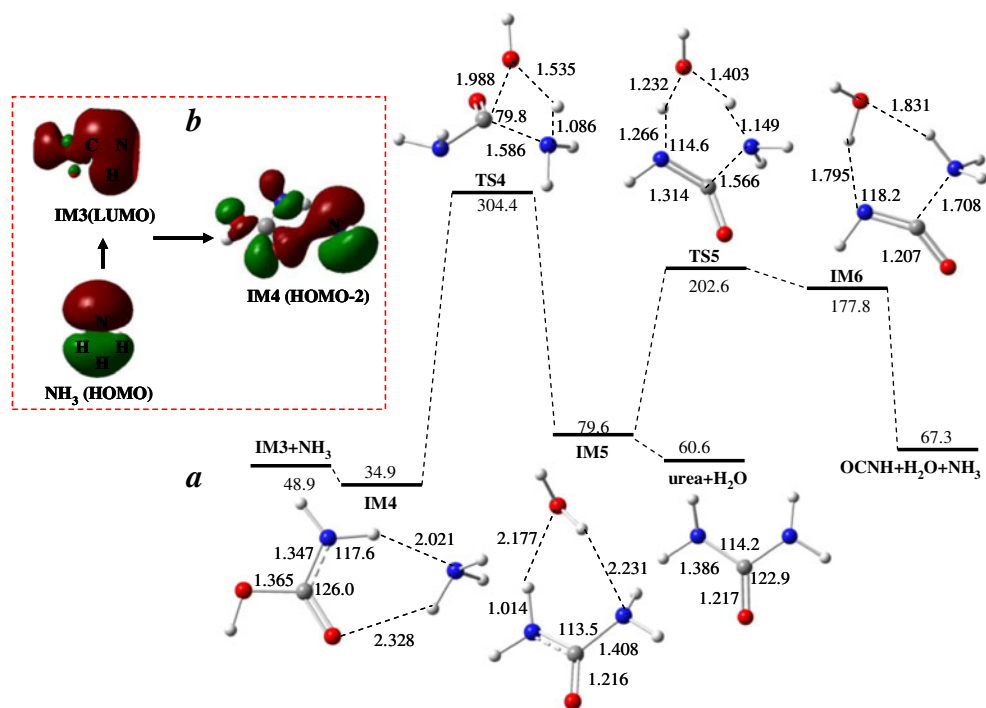


**Fig. 4** PES profiles corresponding to  $\text{urea} + \text{CO}_2$  and  $\text{IM8} + \text{CO}_2$  addition reactions

adding CO<sub>2</sub> to **IM8** to generate **IM10**, followed with adding NH<sub>3</sub> to **IM10** to produce cyanuric acid ultimately.

Reactions of **IM8** + CO<sub>2</sub> → **IM10**,  
and **IM10** + NH<sub>3</sub> → **IM13** → cyanuric acid

As shown in Fig. 4, CO<sub>2</sub> adds to **IM8** to form intermediate **IM9**, and then the imine hydrogen transfers to CO<sub>2</sub> via **TS7** to produce **IM10** with a high barrier of 279.8 kJ/mol<sup>-1</sup>. Similarly, the carboxyl group of **IM10** is amidated by adding CO<sub>2</sub> followed with H-transfer to form **IM12** via **TS8**. In **IM13**, an imine hydrogen atom bonds to the neighboring hydroxyl oxygen to form an eight-membered ring via a hydrogen bond (2.052 Å). The energy barrier is also high (274.0 kJ/mol<sup>-1</sup>) as depicted in Fig. 5. Then **IM13** is cyclized and dehydrated via a hydrogen-shift transition state **TS9** to generate **IM14**, which has been proved by Rác et al. [36]. The free energy barrier is 198.0 kJ/mol<sup>-1</sup>. Subsequently, **IM14** decomposes into cyanuric acid and H<sub>2</sub>O. From the PES profile it can be seen that the products are energetically stable species.

Our calculations predict that the overall reaction 3NH<sub>3</sub> + 3CO<sub>2</sub> → P + 3H<sub>2</sub>O is endothermic with an enthalpic

difference of 71.9 kJ/mol<sup>-1</sup> at 473.15 K and 100 atm. However, the free energy difference Δ*G* (174.8 kJ/mol<sup>-1</sup>) is relatively large, which is attributed to the entropic effect. We investigated whether the sequence of adding NH<sub>3</sub> and CO<sub>2</sub> can determine the potential energy surface (PES).

**IM8** + NH<sub>3</sub> → **IM17**, and **IM17** + CO<sub>2</sub> → **IM19**

As shown in Fig. 6, the energy barriers of adding NH<sub>3</sub> to **IM8** and subsequently adding CO<sub>2</sub> to the generated **IM17** are 251.7 and 268.7 kJ/mol<sup>-1</sup>, respectively. **IM19** is a trans isomer of **IM13**. It can transform to **IM13** via two group-rotation processes and increases its relative free energy by 32.0 kJ/mol<sup>-1</sup>. Obviously, the sequence of adding NH<sub>3</sub> and CO<sub>2</sub> does not influence the free energy barriers.

Our theoretical model reveals that all reaction channels from urea to cyanuric acid bear high barriers. The high pressure and temperature do not decrease Δ*G* and Δ*H* markedly, so, for the formation of cyanuric acid, a one-step mechanism may exist. OCNH can be synthesized from urea [37], and cyanuric acid can be synthesized from OCNH. The dimerization mechanism of OCNH has been investigated [38], where

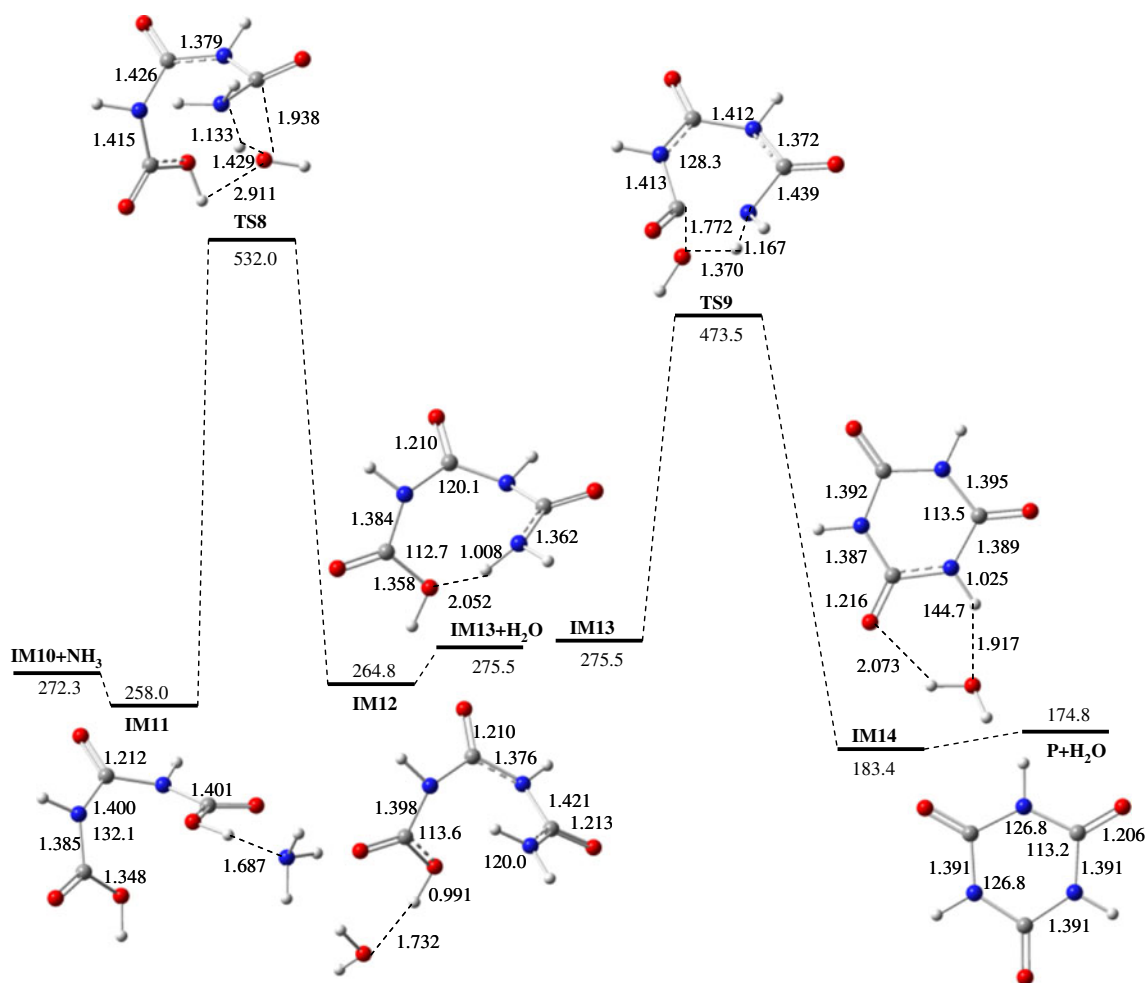


**Fig. 5** Formation of cyanuric acid from **IM10** via **TS8** and **TS9**

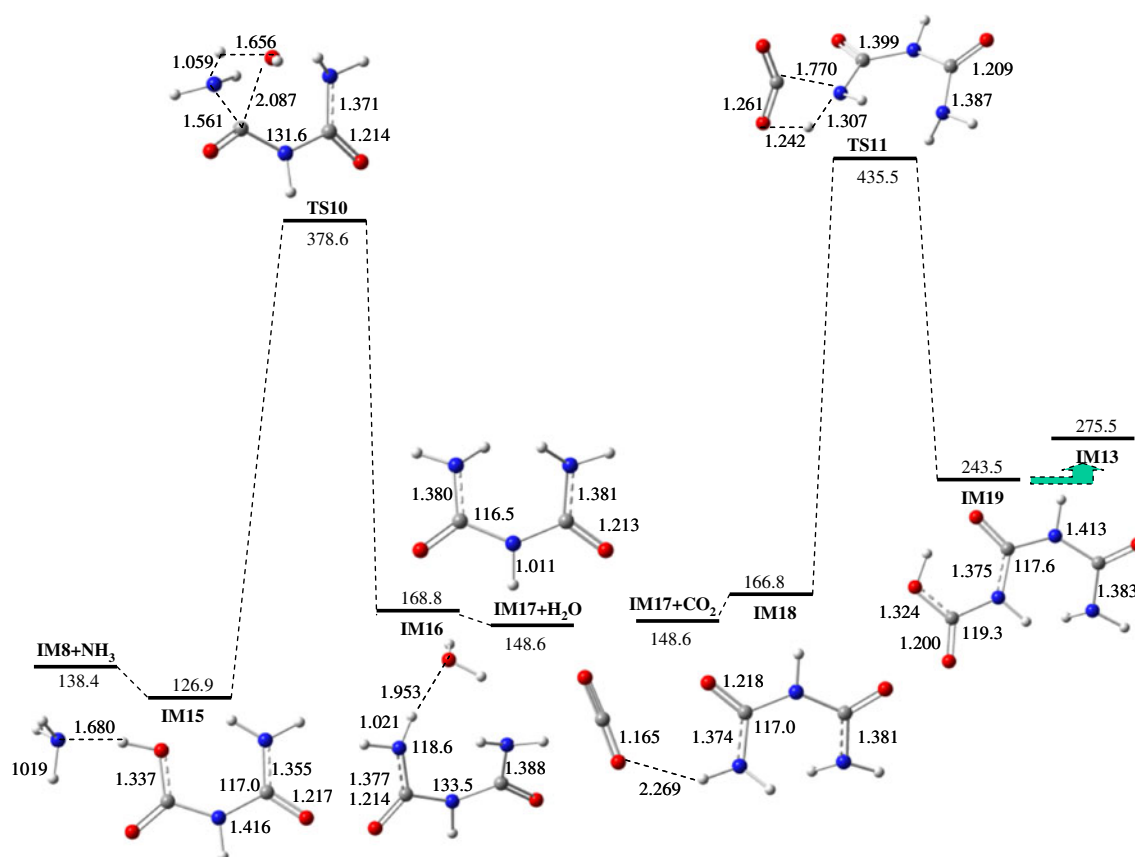


**Fig. 6** Formation of IM19 by adding  $\text{NH}_3$  and  $\text{CO}_2$  to IM8

the stepwise reaction through the cyclic intermediates  $(\text{OCNH})_2$  is unfavorable. Moreover, a one-step synthesis mechanism from  $\text{OCNH}$  has been predicted [15, 19, 30]. We next investigated the cycloaddition reaction of  $\text{OCNH}$  producing cyanuric acid.

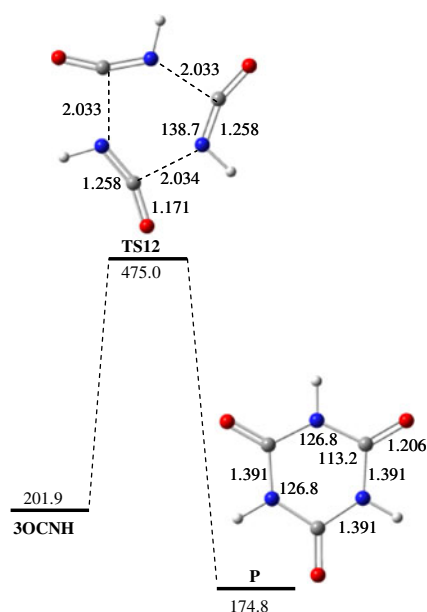


**Fig. 7** One-step synthesis of cyanuric acid from  $\text{OCNH}$

The one-step cycloaddition reaction of cyanuric acid from  $\text{OCNH}$

Three  $\text{OCNH}$  molecules can be cyclized to cyanuric acid (**P**) via **TS12**, as depicted in Fig. 7. The smooth curve from IRC scanning shows that there is no intermediate between  $\text{OCNH}$  and **TS12**. The  $\Delta E$  barrier of this one-step mechanism is only  $168.0 \text{ kJ/mol}^{-1}$ —much lower than those in the stepwise mechanism from urea to **P**—but the free energy barrier ( $273.1 \text{ kJ/mol}^{-1}$ ) does not decrease noticeably. Of course, a one-step synthetic channel with a relatively lower barrier will acquire a higher yield, so this process is energetically more favorable than the multi-step mechanism. Moreover, the relative enthalpies are low, and the high exothermicity may also drive this one-step cycloaddition reaction.

For the total reaction of  $3\text{NH}_3 + 3\text{CO}_2 \rightarrow \text{P} + 3\text{H}_2\text{O}$ , urea or  $\text{OCNH}$  is obtained from  $\text{NH}_3$  and  $\text{CO}_2$ , and then cyanuric acid is cyclized from  $\text{OCNH}$ .

## Conclusions

The synthesis mechanism of cyanuric acid from  $\text{NH}_3$  and  $\text{CO}_2$  was investigated at B3LYP/6-311++G(d,p) level, the condition of 473.15 K and 100 atm was considered with

thermodynamic function calculations in the rigid rotor and harmonic oscillator approximation. In the stepwise mechanism, the module molecules are linked together via weak van der Waals interactions, and then hydrogen transfers to the carboxyl oxygen to form new hydroxyl groups, or transfers to neighboring hydroxyl oxygen to dehydrate the hydroxyl groups; simultaneously new C–N bonds form to ultimately yield cyanuric acid. The addition reactions of NH<sub>3</sub> and CO<sub>2</sub> produce two key intermediates urea and OCNH. However, the energy barriers producing cyanuric acid are generally high in the stepwise mechanism, and the high pressure and temperature do not markedly decrease the thermodynamic values  $\Delta G$  and  $\Delta H$ . Therefore, cyanuric acid is obtained from the cycloaddition reaction of OCNH. In this one-step reaction, the free energy barrier is 273.1 kJ/mol<sup>-1</sup>.

**Acknowledgments** This work was supported by the National Natural Science Foundation of China (No. 21173129 and 11174215), the Natural Science Foundation of Shandong Province, China (No. ZR2012BL10) and the University Science and Technology Project of Shandong Province (No. J13LD05).

## References

- Liang X, Zheng W, Wong N, Li J, Tian A (2004) *J Mol Struct (Theochem)* 672:151–159
- Kobayashi T, Okada A, Fujii Y, Niimi K, Hamamoto S, Yasui T, Tozawa K, Kohri K (2010) *Urol Res* 38:117–125
- Luo Y, Zhang L, Yang W, Liu W, Lu W, Li M (2011) *J Labelled Compd Rad* 54:171–172
- Musumeci D, Ward MD (2011) *CrystEngComm* 13:1067–1069
- Dome JL, Doerge DR, Vandenbroeck M, Fink-Gremmels J, Mennes W, Knutsen HK, Vernazza F, Castle L, Edler L, Benford D (2013) *Toxicol Appl Pharm* 270:218–229
- Pop F, Socaci C, Terec A, Condamine E, Varga RA, Raț CI, Roncali J, Grosu I (2012) *Tetrahedron* 68:8581–8588
- Bahrami K, Khodaei MM, Sohrabnezhad S (2011) *Tetrahedron Lett* 52:6420–6423
- Xue C, Zhu H, Zhang T, Cao D, Hu Z (2011) *Colloids Surf A: Physicochem Eng Aspects* 375:141–146
- Hu A, Zhang F (2010) *J Phys Condens Matter* 22:505402
- Ripka AS, Díaz DD, Sharpless KB, Finn MG (2003) *Org Lett* 5:1531–1533
- Tsipis CA, Karipidis PA (2003) *J Am Chem Soc* 125:2307–2318
- Vinogradova EV, Fors BP, Buchwald SL (2012) *J Am Chem Soc* 134:11132–11135
- Kanno E, Yamanoi K, Koya S, Azumaya I, Masu H, Yamasaki R, Saito S (2012) *J Org Chem* 77:2142–2148
- Wu C, Cheng H, Liu R, Wang Q, Hao Y, Yu Y, Zhao F (2010) *Green Chem* 12:1811–1816
- Seifer GB (2002) *Russ J Coord Chem* 28:301–324
- Tsipis CA, Karipidis PA (2005) *J Phys Chem A* 109:8560–8567
- She D, Yu H, Huang Q, Li F, Li C (2010) *Molecules* 15:1898–1902
- Piazzesi G, Kröcher O, Elsener M, Wokaun A (2006) *Appl Catal B: Environ* 65:55–61
- Geith J, Klapötke TM (2001) *J Mol Struct (Theochem)* 538:29–39
- Bernhard AM, Peitz D, Elsener M, Wokaun A, Kröcher O (2012) *Appl Catal B: Environ* 115–116:129–137
- Tang H, Doerksen RJ, Tew GN (2005) *Chem Commun* 12:1537–1539
- Wells GM, Dudding T, Belding L, Frick JA, Nayek A, Huang J, Katz SJ, Bergmeier SC (2012) *Tetrahedron* 68:3980–3987
- Li TH, Wang CM, Xie XG, Du GB (2012) *J Phys Org Chem* 25:118–125
- Nowacki A, Sikora K, Dmochowska B, Wiśniewski A (2013) *J Mol Model*. doi:10.1007/s00894-013-1835-7
- Frisch MJ, Trucks GW, Schlegel HB, Scuseria GE, Robb MA, Cheeseman JR, Zakrzewski VG, Montgomery JA, Stratmann RE, Burant JC, Dapprich S, Millam JM, Daniels AD, Kudin KN, Strain MC, Farkas O, Tomasi J, Barone V, Cossi M, Cammi R, Mennucci B, Pomelli C, Adamo C, Clifford S, Ochterski J, Petersson GA, Ayala PY, Cui Q, Morokuma K, Malick DK, Rabuck AD, Raghavachari K, Foresman JB, Cioslowski J, Ortiz JV, Stefanov B, Liu G, Liashenko A, Piskorz P, Komaromi I, Gomperts R, Martin RL, Fox DJ, Keith T, Al-Laham MA, Peng CY, Nanayakkara A, Gonzalez C, Challacombe M, Gill PMW, Johnson BG, Chen W, Wong MW, Andres JL, Head-Gordon M, Replogle ES, Pople JA; Gaussian 03, revision C.02 (2004) Gaussian Inc; Wallingford CT
- Cheng X, Chen D, Liu Y (2012) *Chem Phys Chem* 13:2392–2404
- Head-Gordon M, Pople JA, Frisch M (1988) *Chem Phys Lett* 153:503–506
- Gonzalez C, Schlegel HB (1990) *J Phys Chem* 94:5523–5527
- Gonzalez C, Schlegel HB (1989) *J Chem Phys* 90:2154–2161
- Fang D, Fu X (1996) *J Mol Struct (Theochem)* 365:219–223
- Wei X, Sun X, Wu X, Geng S, Ren Y, Wong N, Li W (2011) *J Mol Model* 17:2069–2082
- Zabardasti A, Solimannejad M (2007) *J Mol Struct (Theochem)* 819:52–59
- Rode JE, Dobrowolski JC (2006) *J Phys Chem A* 110:3723–3737
- Zhang X, Geng Z (2010) *J Mol Struct (Theochem)* 955:33–38
- Zabardasti A, Amani S, Solimannejad M, Salehnassaj M (2009) *Struct Chem* 20:1087–1092
- Rácz Á, Váradi A, Mazák K, Kőkösi J, Noszál B (2013) *J Mol Model*. doi:10.1007/s00894-013-1905-x
- Czekaj I, Kröcher O, Piazzesi G (2008) *J Mol Catal A Chem* 280:68–80
- Feng W, Wang Y, Zhang S (1995) *J Mol Struct (Theochem)* 342:147–151